of available states in the ground state (ground state entropic loss) or by increasing the number of available states at the transition state (transition state entropic gain). In LDH, the hydride transfer reaction follows a fairly precise reaction pathway, and the reaction coordinate involves nicotinamide's C4-H bond and substrate's C=O bond.[40] Entropy must be lost to bring together the C4-H bond of NADH and the C=O bond of pyruvate with the right orientation for the reaction to proceed. If this entropy loss is already realized in the LDH·NADH·pyruvate complex, as evidenced by our Raman results, it need not be done in the transition state, and the catalytic capability of LDH would be enhanced. It seems reasonable to suppose that the ground state entropic loss for the C4-H and C=O coordinates suggested by our data and calculations is expressed as a decrease of the barrier in the reaction pathway. This is the same as assuming that the conformations observed in the binary complex are nonproductive except for the conformation picked out upon the formation of the ternary complex which is structured properly for reaction. Assuming this to be true, this analysis suggests that of the 4.2 kcal/mol lowering of the transition state barrier upon loop closure found by Holbrook and co-workers,[1] some 1.4 kcal/mol arises from a raising of the ground state free energy relative to the transition state from entropic effects.

(44) Page, M. I.; Jencks, W. P. *Proc. Natl. Acad. Sci. U.S.A.* **1971**, *68*, 1678-1683.

(+)-Hitachimycin: Stereochemistry and Conformational Analysis

Amos B. Smith, III,*,‡ John L. Wood,‡ Carmelo J. Rizzo,‡ George T. Furst,‡ Patrick J. Carroll,‡ Jerry Donohue,†,‡ and Satoshi Ōmura§

Contribution from the Department of Chemistry, Monell Chemical Senses Center, and Laboratory for Research on the Structure of Matter, University of Pennsylvania, Philadelphia, Pennsylvania 19104, and School of Pharmaceutical Sciences, Kitasato University, and Kitasato Institute, Minato-ku, Tokyo 108, Japan. *Received April 1, 1992*

Abstract: The complete relative and absolute stereochemistry and the solid-state and solution conformations of (+)-hitachimycin (a.k.a. stubomycin) (**1**) have been defined via NMR experiments, single-crystal X-ray analysis, and computational methods.

In the early 1980s, Ōmura[1] and Umezawa[2] independently isolated the macrocyclic antitumor antibiotic (+)-hitachimycin (a.k.a. stubomycin) (**1**) from an unidentified *Actinomycetes* strain (MK-4927) and from *Streptomyces* sp. KG-2245, respectively. Whereas the Ōmura group focused primarily on structure elucidation, Umezawa and co-workers demonstrated the cytotoxicity of **1** against Ehrlich ascites carcinoma, P388 lymphocytic leukemia, and HeLa S_3 cells.[1-4] Our interest in (+)-**1** stemmed from both its novel architecture and its reported anticancer activity. Herein we describe the elucidation of the relative and absolute stereochemistry and the solid-state and solution conformations of **1**. In the following article in this issue, we detail the first (and to date only) total synthesis of (+)-**1**.

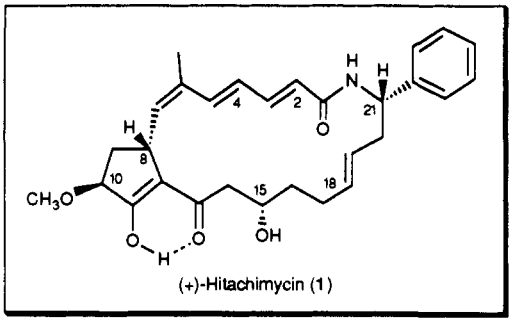

Ōmura Degradation Studies: Absolute Configurations of C(15) and C(21). Degradation experiments by Ōmura et al. had established the *S* absolute stereochemistry at both C(15) and C(21). Specifically, ozonolysis followed by oxidative workup, acidification, and esterification (CH_2N_2) provided three degradation products: (*S*)-(+)-tetrahydro-5-oxo-2-furanacetic acid methyl ester (**2**) and urethanes **3** and **4**. Hydrolysis of **3** and **4** with aqueous HCl afforded a single compound, which proved to be (*S*)-(+)-β-phenyl-β-alanine (**5**). Importantly, the absolute configurations of (+)-**2** and (+)-**5** had been established via earlier syntheses.[5,6]

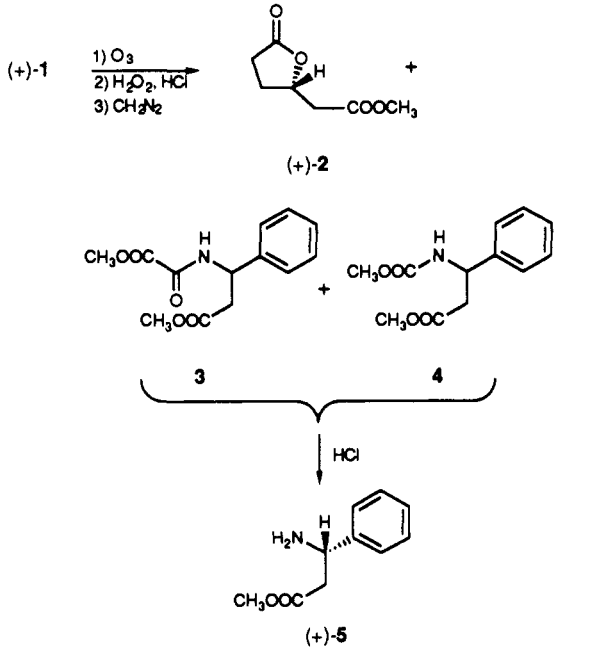

X-ray Analysis of (+)-Hitachimycin (1). In an effort to assign the relative and absolute stereochemistry at the remaining centers [i.e., C(8) and C(10)], we collected a complete set of X-ray diffraction data; refinement yielded a structure with an *R* value

† Deceased February 13, 1985.
‡ University of Pennsylvania.
§ Kitasato Institute.

0002-7863/92/1514-8003$03.00/0

of 12.8% (Figure 1). Given the high value of R,[7] which derived from the unexpected inclusion of two disordered chloroform molecules in the unit cell,[8] this analysis was considered to provide only a tentative stereochemical assignment. Interestingly, inspection of pertinent atomic distances and calculation of the best plane through the five-membered ring suggested the presence of an enolic cyclopentene moiety (Figure 2). Carbons 8 and 10–12 were coplanar, whereas C(9) was displaced from the plane by 0.513 Å.

The inconclusive crystallographic analysis dictated further investigation of the structure of (+)-**1** before valuable scalemic material was committed to the construction of the subunit containing C(8) and C(10). We envisioned that NMR and computational studies would provide needed support for the crystal structure as well as an accurate representation of the solution conformation.[9] Accordingly, we initiated a multifaceted effort directed toward (A) probing the existence of a predominant solution conformation (i.e., conformational homogeneity), (B) measurement of ^{1}H NMR vicinal coupling constants, (C) determination of intramolecular atomic proximities via NOE studies, and (D) elucidation of the solution conformation via comparison of the experimental coupling constants and NOE data with calculated values for the minimum-energy conformers and the conformation observed via X-ray analysis.

The Question of Conformational Homogeneity. Before elucidating the solution conformation of (+)-hitachimycin, we had to establish that **1** exists as a single conformer or family of closely related conformers. Conformational homogeneity is a central consideration in conformational analysis and, particularly in the peptidyl area, numerous NMR criteria are regarded as indicative.[10] Those applicable to non-peptides include (1) large chemical shift differences between diastereotopic geminal protons, (2) vicinal coupling constants varying significantly from the average of ca. 7.5 Hz, and (3) little or no dependence of the coupling constants upon the solvent or temperature.

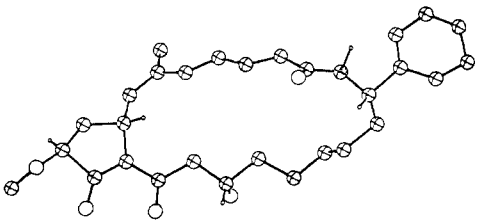

Figure 1. ORTEP drawing of crystalline **1**.

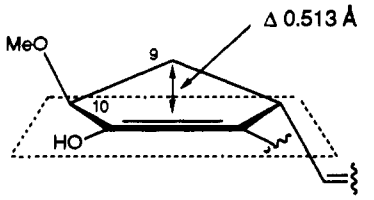

Figure 2. Calculated best plane through the cyclopentenoid moiety.

Table I. ^{1}H and ^{13}C NMR Chemical Shift Assignments for (+)-**1**

position	^{13}C chemical shift (δ)	^{1}H chemical shift (δ)
C(1)	166.04	
C(2)	123.80	5.87
C(3)	141.61	7.26
C(4)	127.39	6.35
C(5)	136.75	7.01
C(6)	131.05	
C(7)	134.82	5.17
C(8)	34.91	3.95
C(9)	35.36	2.06, 2.06
C(10)	80.70	4.43
C(12)	112.22	
C(14)	46.48	2.36, 2.05
C(15)	67.65	3.89
C(16)	38.91	1.22, 1.08
C(17)	29.21	2.27, 1.87
C(18)	134.11	5.37
C(19)	126.37	5.47
C(20)	41.43	2.69, 2.12
C(21)	51.66	5.29

Table II. Coupling Constants for (+)-**1** Determined by 1D Techniques

nuclei	J value (Hz)	nuclei	J value (Hz)
H(2)–H(3)	14.9	H(9a)–H(10)	7.6
H(3)–H(4)	11.1	H(9b)–H(10)	7.6
H(4)–H(5)	15.3	H(14a)–H(15)	1.5
H(7)–H(8)	10.9	H(14b)–H(15)	11.4
H(8)–H(9a)	5.2	H(14a)–H(14b)	17.4
H(8)–H(9b)	5.2	NH–H(21)	10.1

As evaluation of the first two criteria requires detailed analysis of the ^{1}H NMR spectrum, we initially sought to verify both the ^{1}H and ^{13}C chemical shift assignments originally reported for (+)-**1**.[1b] A combination of COSY (^{1}H–^{1}H) and HETCORR (^{1}H–^{13}C) two-dimensional experiments (Table I) confirmed the reported values.[11] Importantly, this analysis also revealed distinctly different chemical shifts for all of the diastereotopic protons within the macrocyclic ring [i.e., H(14a,b), H(16a,b), H(17a,b), and H(20a,b)], consistent with conformational homogeneity.[12] Variable-temperature ^{1}H NMR experiments over a 110 °C range ($CDCl_3$ solvent, −50 → 60 °C) were likewise suggestive of conformational homogeneity. Low temperature slowed the exchange of the vinylogous acid and secondary hydroxyl hydrogens,

(1) (a) Ōmura, S.; Nakagawa, A.; Tanaka, Y. In *Trends in Antibiotic Research*; Umezawa, H., Ed.; Japan Antibiotics Research Association: Tokyo, 1982; pp 135–145. (b) Ōmura, S.; Nakagawa, A.; Shibata, K.; Sano, H. *Tetrahedron Lett.* **1982**, *23*, 4713.

(2) Umezawa, I.; Takeshima, H.; Komiyama, K.; Koh, Y.; Yamamoto, H.; Kawaguchi, M. *J. Antibiot.* **1981**, *34*, 259.

(3) Komiyama, K.; Edanami, K.; Yamamoto, H.; Umezawa, I. *J. Antibiot.* **1982**, *35*, 703.

(4) For recent studies on the biological activity of hitachimycin analogs, see: (a) Shibata, K.; Satsumabayashi, S.; Sano, H.; Komiyama, K.; Nakagawa, A.; Ōmura, S. *J. Antibiot.* **1988**, *41*, 614. (b) Shibata, K.; Satsumabayashi, S.; Sano, H.; Komiyama, K.; Zhi-Bo, Y.; Nakagawa, A.; Ōmura, S. *J. Antibiot.* **1989**, *42*, 718. (c) Shibata, K.; Satsumabayashi, S.; Sano, H.; Komiyama, K.; Zhi-Bo, Y.; Nakagawa, A.; Ōmura, S. *J. Antibiot.* **1989**, *42*, 1114.

(5) (a) Kato, Y.; Wakabayashi, T. *Synth. Commun.* **1977**, 125. (b) Wakabayashi, T.; Kato, Y. *Heterocycles* **1977**, *6*, 395.

(6) Wasserman, H. H.; Berger, G. D. *Tetrahedron* **1983**, *39*, 2459.

(7) Although suitable for tentative assignment of the relative stereochemistry, this R value is about 50% larger than is currently acceptable.

(8) Although we attempted to crystallize the hitachimycin from a variety of solvent systems, none of the resultant crystals proved superior to one found in the amorphous powder kindly provided by Professor Ōmura.

(9) For solution conformation studies in other macrocyclic systems, see the following. (a) Peptides: Bruch, M. D.; Noggle, J. H.; Gierasch, L. M. *J. Am. Chem. Soc.* **1985**, *107*, 1400. Glickson, J. D.; Gordon, S. L.; Pitner, T. P.; Agresti, D. G.; Walter, R. *Biochemistry* **1976**, *15*, 5721. Kessler, H.; Bats, J. W.; Griesinger, C.; Koll, S.; Will, M.; Wagner, K. *J. Am. Chem. Soc.* **1988**, *110*, 1033. (b) Nonpeptides: Everett, J. R.; Tyler, J. W. *J. Chem. Soc., Perkin Trans. 2* **1987**, 1659. Baker, G. H.; Brown, P. J.; Dorgan, R. J. J.; Everett, J. R.; Ley, S. V.; Slawin, A. M. Z.; Williams, D. G. *Tetrahedron Lett.* **1987**, *28*, 5565. Cellai, L.; Cerrini, S.; Segre, A.; Brufani, M.; Fedeli, W.; Vaciago, A. *J. Org. Chem.* **1982**, *47*, 2652. Arora, S. K.; Kook, A. M. *J. Org. Chem.* **1987**, *52*, 1530. Radics, L.; Incze, M.; Dornberger, K.; Thrum, H. *Tetrahedron* **1982**, *38*, 183. Sugiura, M.; Beierbeck, H.; Bélanger, P. C.; Kotovych, G. *J. Am. Chem. Soc.* **1984**, *106*, 4021. Kam, M.; Shafer, R. H.; Berman, E. *Biochemistry* **1988**, *27*, 3581. (c) Effects of conformation on chemical reactivity: Still, W. C.; Galynker, I. *Tetrahedron* **1981**, *37*, 3981. Still, W. C. In *Current Trends in Organic Synthesis*; Nozaki, H., Ed.; Pergamon: New York, 1982; p 233. Still, W. C. *J. Am. Chem. Soc.* **1979**, *101*, 2493.

(10) (a) Kessler, H.; Bermel, W. In *Methods in Stereochemistry Analysis*; Takeuchi, V., Marchand, A. P., Eds.; VCH Publishers: Deerfield Beach, FL, 1986; Vol. 6, p 179. (b) Kessler, H. *Angew. Chem., Int. Ed. Engl.* **1982**, *21*, 512.

(11) A complete listing of proton and carbon chemical shift assignments is provided as supplementary material.

(12) Herein protons are labeled in accord with the carbon numbering. The letter "a" (e.g., H(16a)) designates the downfield resonance of a diastereomeric pair; H(16b) would refer to the upfield resonance of the C(16) methylene.

Table III. DISCO-Derived Coupling Constants for H(16a)

spin system	*J* value (Hz)
H(16a)–H(15) + H(16a)–H(17b)	22.7[a]
H(16a)–H(16b)	13.8[b]
H(16a)–H(17a)	3.7[c]

[a] Single value: [(632.7 + 628.8 + 618.6 + 615.3)/4] – [(610.1 + 606.1 + 596.1 + 592.3)/4] = 22.7. [b] Average of two values: [(632.7 + 628.8)/2 – (618.6 + 615.3)/2] = 13.8; [(610.1 + 606.1)/2 – (596.1 + 592.3)/2] = 13.8; (13.8 + 13.8)/2 = 13.8. [c] Average of four values: 632.7 – 628.8 = 3.8; 618.6 – 615.3 = 3.2; 610.1 – 606.1 = 4.0; 596.1 – 592.3 = 3.8; (3.8 + 3.2 + 4.0 + 3.8)/4 = 3.7.

whereupon these previously unresolved resonances appeared as broad singlets at δ 12.9 and 2.7, respectively. Whereas conformational mobility of the cyclopentenoid unit became apparent at temperatures near −50 °C, as evidenced by significant changes in the C(8) and C(9) proton signals, the C(10) proton resonance and the $J_{7,8}$ coupling constant showed no temperature dependence. Experiments performed in $CDCl_3/CD_3OD$ (4:1) also pointed toward a conformationally homogeneous macrocyclic ring.

Determination of Vicinal Coupling Constants. To evaluate the second criterion for conformational homogeneity and to obtain additional data indicative of the solution conformation, we next sought to determine all nonaromatic vicinal coupling constants. Both 1D and 2D NMR techniques were employed. An initial review of the 1D proton spectrum led to unambiguous assignment of the coupling constants associated with the protons at the 2–5, 7–10, and 14a positions and the NH proton (Table II). Homonuclear decoupling then furnished $J_{8,9a}$ and $J_{8,9b}$; upon irradiation of the H(7) vinyl proton at δ 5.17, the H(8) resonance collapsed to a broad, apparent triplet with 5.2 Hz couplings for both H(8)–H(9a) and H(8)–H(9b).

We further exploited the arsenal of one-dimensional techniques by irradiating the H(15) multiplet at δ 3.89 to probe the H(14a,b) resonances. Although the region containing the H(14b) signal (near δ 2.05) seemed hopelessly convoluted, the difference method[13] proved successful, confirming the previously established 17.4 Hz geminal coupling of the C(14) diastereotopic protons and also revealing an 11.4 Hz coupling of H(15) and H(14b). A complete listing of the coupling constants derived from 1D methods appears in Table II.

Having compiled all of the coupling constants discernible via 1D techniques, we turned to double-quantum-filtered, two-dimensional, phase-sensitive COSY experiments (DQFCOSYPH).[14] An initial spectrum of the entire chemical shift range (i.e., δ 7.7–0.7) verified the earlier proton assignments, but the resolution did not furnish accurate coupling constant measurements. To enhance the digital resolution while maintaining data sets of manageable size, we performed two additional DQFCOSYPH experiments with narrower sweep widths: δ 1.8–5.5 and 0.9–5.0. The latter parameters were chosen to ensure that the foldback of outlying resonances would not interfere with the regions of interest. For analysis of the 2D, phase-sensitive COSY data,[15] the DISCO technique was applied to appropriate f-2 cross-peak projections. This recently developed method reduced the cross-peak multiplicities by a factor of 2, thereby solving the propinquity problem of the antiphase peaks and providing accurate coupling constants.[16]

Of the spin systems requiring assignment via 2D techniques, the more complex were methylenes H(16a,b) (δ 1.22 and 1.08, respectively) and H(17a,b) (δ 2.27 and 1.87), wherein each proton is coupled to four spins. To unravel these coupling networks, as well as those derived from H(15) and H(18), we examined numerous cross peaks via the DISCO technique. We initially focused

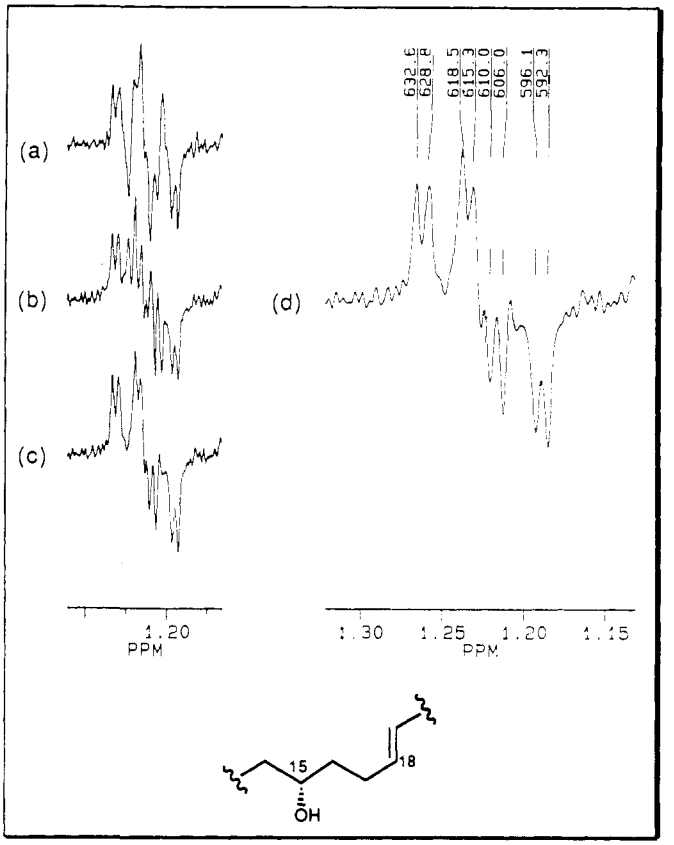

Figure 3. F-2 projections of the cross peaks H(16a) × H(15) (a) and H(16a) × H(17b) (b) and the sum thereof (c and d). Chemical shift data (hertz) appear above the expanded segment (d).

Table IV. Coupling Constants for (+)-**1** Derived via 2D Techniques

nuclei	*J* values (Hz)[a]	nuclei	*J* values (Hz)
H(15)–H(16a)	9.7, 10.0, 9.9 (9.9)	H(17a)–H(18)	4.2
H(15)–H(16b)	2.2, 2.3 (2.2)	H(17b)–H(18)	9.1
H(16a)–H(16b)	13.8, 13.9 (13.9)	H(18)–H(19)	15.5
H(16a)–H(17a)	3.7, 3.8, 3.9 (3.8)	H(19)–H(20a)	3.8
H(16b)–H(17a)	13.5, 13.3 (13.4)	H(19)–H(20b)	9.8, 9.5 (9.63)
H(16a)–H(17b)	12.7	H(20a)–H(20b)	13.8
H(16b)–H(17b)	4.9	H(20a)–H(21)	2.8
H(17a)–H(17b)	12.9	H(20b)–H(21)	11.2

[a] Averages are listed parenthetically.

on H(16a) × H(15) and H(16a) × H(17b);[17] the DISCO projections and the sum of these cross peaks are illustrated in Figure 3. As expected, addition reduced the 16-line pattern of the H(16a) multiplet to a more manageable 8-line doublet of doublet of doublets. From the distance between the centers of the antiphase multiplets,[16] we determined the sum of the H(16a)–H(15) and H(16a)–H(17b) coupling constants (Table III). Likewise, the two coupling constants manifest in the in-phase portion of the summed data were readily discernible. As only one of the latter *J* values reflected a geminal relationship, the H(16a)–H(16b) and H(16a)–H(17a) couplings were readily distinguished (13.8 and 3.7 Hz, respectively). Similar analyses of the remaining 2D cross peaks led to the assignment of the vicinal coupling constants outlined in Table IV.

Coupling Constant Determination and Verification via PANIC Simulation. The aforementioned 1D and 2D techniques furnished all but the H(9a)–H(9b) coupling constant. Although this *J* value was not required for conformational analysis of the macrocyclic portion of (+)-**1**, we nonetheless attempted to ascertain an appropriate value via simulation. The latter exercise was also expected to confirm our earlier coupling constant measurements.

(13) Sanders, J. K. M.; Mersh, J. D. In *Progress in NMR Spectroscopy*; Emsley, J. W., Feeney, J., Sutcliffe, L. H., Eds.; Pergamon: New York, 1982; Vol. 15, pp 353–400.
(14) For leading references, see: Wemmer, D. E. *Concepts Magn. Reson.* **1989**, *1*, 59.
(15) Ernst, R. R. *Chimia* **1987**, *41*, 323.
(16) Kessler, H.; Muller, A.; Oschkinat, H. *Magn. Reson. Chem.* **1985**, *23*, 844.
(17) The notation H(16a) × H(15) refers to the cross peak derived from the H(16a) and H(15) resonances. The resonance listed first (i.e., H(16a)) is from the f-2 dimension and the second from the f-1 dimension.

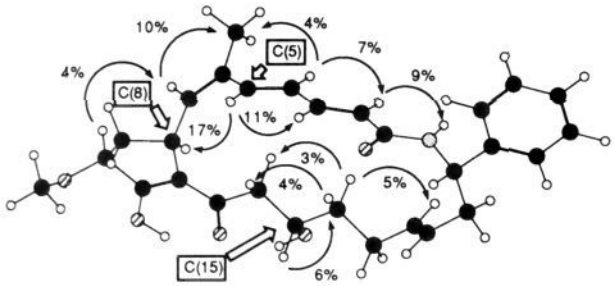

Figure 4. NOE data for (+)-**1**, illustrated on a drawing of the X-ray structure.

Indeed, by employing the experimental coupling constants and chemical shifts as variables without iterative adjustment, the simulation program PANIC generated a nearly perfect reproduction of the ^{1}H NMR spectrum.[18] Interactive adjustment then revealed that a low $J_{9a,9b}$ value of 0.24 Hz best matched the experimental data;[19] this anomalous result again reflects the conformational mobility of the cyclopentenoid moiety (vide supra).

NOE Experiments. The vicinal coupling constants significantly diverged from the mean of 7.5 Hz, suggesting a high degree of conformational homogeneity for the hitachimycin macrocyclic skeleton. Confident, then, that the experimental NMR data reflected a predominant solution conformation, we undertook an extensive nuclear Overhauser enhancement (NOE) study. The NOEDIFF microprogram supplied with the Bruker NMR software package was employed.[20] This exercise established the proximity of numerous nuclei, illustrated via a representation of the X-ray conformation in Figure 4. Of particular interest are the proximities of H(5)–H(8) (17% enhancement), which establish an orthogonal disposition of the C(1–7) olefinic bridge toward the cyclopentene ring, and of H(16a)–H(18) (5%), indicative of a staggered orientation of the isolated ethylene unit relative to the C(16) methylene group. In addition, the NOEs involving H(14a)–H(16b) (4%) and H(14b)–H(16a) (3%) suggest a "zigzag" conformation in the aliphatic chain. Interestingly, the NOE data are accommodated quite well by the conformation found in the X-ray structure as shown. The close correspondence of the X-ray and solution conformations is also manifest in the corresponding vicinal coupling constants (vide infra).

Comparison of Computational and Experimental Coupling Constants. Upon the successful compilation of coupling constants and NOE data, we turned to computer-aided conformational analysis. Two methods, Multiconformer[21] and Monte Carlo,[22] were employed for global conformational searching; both were developed by Still and are incorporated into the MacroModel molecular modeling package.[23]

Following prescribed procedures,[21] we carried out a Multiconformer search employing a 0.1 → 5 Å closure bond between C(20) and C(21). All single bond torsion angles unique to the macrocycle were varied in 60° increments; following elimination of duplicate structures, over 200 unique conformations remained. Partial minimization of the latter followed by complete minimization of the 20 lowest energy conformations afforded five unique structures with energies within 3.0 kcal/mol of the global minimum.

Next we utilized the Monte Carlo method.[22] As in the Multiconformer search, a C(20,21) closure bond distance of 0.1 → 5.0 Å was chosen, and all single bonds unique to the macrocycle were allowed to rotate full circle (i.e., 360°). The absence of a restart option in the early version of MacroModel (Batchmin V. 2.6) limited the number of structures that could be generated and minimized; hence, a completely converged Monte Carlo search, as defined by Still,[24] was never realized. Nonetheless, over 3000 conformations were generated. Of these, 1430 proved to be unique and were further minimized, affording seven within 2.5 kcal/mol of the minimum. Importantly, the lowest energy conformation in the latter search was identical to that obtained by the Multiconformer method. Vicinal coupling constants[25] and intramolecular atomic distances were then calculated for the 12 local

Table V. Superimpositions of the X-ray Conformer on the Computational Local Minima

MM2 energy (kcal)	search method	overlap deviation (Å)
0.00	Monte Carlo and Multiconformer	0.281
1.02	Multiconformer	1.650
1.25	Monte Carlo	1.929
1.45	Monte Carlo	1.668
1.54	Monte Carlo	1.823
1.85	Monte Carlo	0.858
1.87	Monte Carlo	1.574
2.11	Monte Carlo	2.143
2.11	Multiconformer	1.347
2.25	Monte Carlo	1.714
2.51	Multiconformer	0.929
2.81	Multiconformer	0.855

Table VI. Correlation Coefficients (R Values) for Comparison of the Experimental Coupling Constants with J Values Calculated for the Computational Local Minima

MM2 energy (kcal/mol)	R value	MM2 energy (kcal/mol)	R value
0.00	0.98	1.87	0.40
1.02	0.38	2.11	0.11
1.25	0.32	2.11	0.31
1.45	0.32	2.25	0.77
1.54	0.76	2.51	0.96
1.85	0.30	2.82	0.29

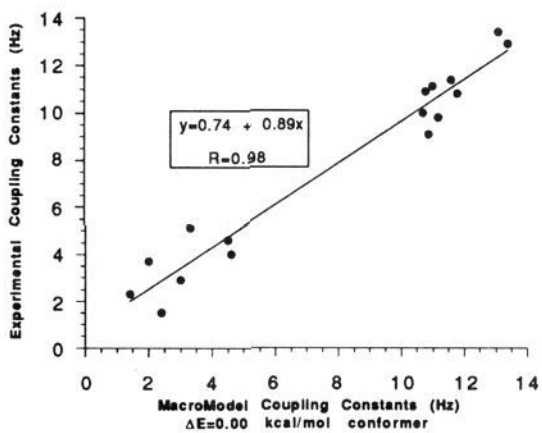

Figure 5. Linear regression analysis comparing the experimentally and computationally (ΔE = 0.00 kcal/mol conformer) derived coupling constants.

(18) (a) The PANIC simulation program is supplied by Bruker Instruments as part of their standard NMR software package. Specifically, it comprises a microcomputer version of LAOCOON 3,[20b] designed to run on the ASPECT computer. (b) Castellano, S.; Bothner-By, A. A. *J. Chem. Phys.* **1964**, *41*, 3863.

(19) A plot of the simulated spectrum is provided as supplementary material.

(20) (a) The 1988 release of Bruker's NMR software, DISNMR88, with the program NOEDIFF.AU was employed. (b) See Neuhaus, D.; Williamson, M. *The Nuclear Overhauser Effect in Structural and Conformational Analysis*; VCH: New York, 1989; pp 211 for a discussion of the technique.

(21) Lipton, M.; Still, W. C. *J. Comput. Chem.* **1988**, *9*, 343.

(22) Chang, G.; Guida, W. C.; Still, W. C. *J. Am. Chem. Soc.* **1989**, *111*, 4379.

(23) Still, W. C.; Mohamadi, F.; Richards, N. G. J.; Guida, W. C.; Lipton, M.; Liskamp, R.; Chang, G.; Hendrickson, T.; DeGunst, F.; Hasel, W. MacroModel V2.5, Department of Chemistry, Columbia University, New York, NY 10027.

(24) Still suggests continuation of the Monte Carlo conformational search until each conformation has been generated five times. Our search was limited by the availability of uninterrupted computer time (ca. 600 h).

(25) Haasnoot, C. A. G.; de Leeuw, F. A. A. M.; Altona, C. *Tetrahedron* **1980**, *36*, 2783.

Table VII. Calculated Coupling Constants for the C(15) and C(18) Methylenes in the ΔE = 0.00 and 2.51 kcal/mol Conformers

protons	J for ΔE = 0.00 conformer	J for ΔE = 2.51 conformer
H(15)–H(16, *pro-R*)	1.4	11.4
H(15)–H(16, *pro-S*)	11.2	3.8
H(18)–H(17, *pro-R*)	10.9	2.6
H(18)–H(17, *pro*-S)	4.5	10.3

minima via the analyze submode of MacroModel.

To compare the NMR, X-ray, and computational results, we then exploited three techniques embodied in the MacroModel program. Rigid superimposition[26] was initially employed to compare the computational minimum energy conformers with the conformation found in the X-ray structure. RMS deviations obtained from the least-squares analyses are listed in Table V. The best fit (0.281 Å deviation) was obtained by overlap of the global minimum and X-ray conformers. The calculated structure affording the next smallest overlap deviation proved to be 2.82 kcal/mol higher in energy.

We then employed linear regression analyses for comparison of the computed coupling constants with those observed by NMR. The analysis for the global minimum is plotted in Figure 5, and the complete results appear in Table VI.[27] Interestingly, excellent correlations with the experimental data were obtained for both the ΔE = 0 (R = 0.98) and ΔE = 2.51 (R = 0.96) conformers. Superimposition revealed that the X-ray and ΔE = 2.51 conformers differ primarily by ca. 109° rotations of the C(15,16) and C(17,18) bonds; the C(16,17) torsion angles are essentially equal. These rotations generate H–C–C–H dihedral angles which are nearly equal in magnitude, though of opposite chirality (Table VII), leading to good correlations of coupling constants for both conformers with the experimental values.

Importantly, evaluation of the experimental NOE data in relation to calculated interatomic distances provides further evidence that the solution structure of **1** closely resembles the global minimum rather than the ΔE = 2.51 conformer. The H(14a)–H(16b) and H(14b)–H(16a) separations are 2.50 and 2.54 Å in the former (ΔE = 0) conformer and 3.89 and 2.52 Å in the latter.[28] As 3.89 Å closely approaches the limit (ca. 4 Å) for observation of an NOE in small molecules, the ΔE = 2.51 structure is incompatible with the observed 4% enhancement.[29] Moreover, the enhancements observed for H(14a)–H(16b) and H(14b)–H(16a) (i.e., 4 and 3%, respectively) are in full accord with the interatomic distances calculated for the minimum energy conformer.

Conclusion. The consistency of the experimental coupling constants and NOE data with calculated values for the computational global minimum and the X-ray conformation strongly suggests that the solution, computational, and crystalline conformers of **1** are essentially identical. This finding buttressed our tentative X-ray crystal structure, allowing us to initiate synthetic efforts with considerable confidence in our structural and stereochemical assignments for (+)-hitachimycin (**1**). A full account of the first total synthesis of **1** appears as the following article in this issue.

(26) (a) See ref 23. (b) Kabsch, W. *Acta Crystallogr.* **1976**, *A32*, 922.

(27) The calculated coupling constants for diastereotopic hydrogens were matched with the corresponding experimental values to give the best fit. Only couplings that MacroModel could match with an appropriate Karplus equation were calculated. Those associated with the C(9) methylene were not utilized in consequence of the conformational mobility of the cyclopentene moiety (vide supra).

(28) The "a" and "b" assignments were based upon the calculated vicinal coupling constants and are consistent with the experimental data.

(29) See ref 20b, p 51.

Experimental Section

General Procedures. NMR spectra were measured using a Bruker AM-500 spectrometer equipped with either a proton only or a proton–carbon dual probe and a standard Bruker variable-temperature unit. Samples were prepared by dissolving ca. 2.0 mg of hitachimycin in 0.5 mL of $CDCl_3$. For NOE studies, a similarly prepared solution was degassed via three freeze–pump–thaw cycles; the percent enhancement was determined by subtraction of the on-resonance from the off-resonance spectra in the dual display mode followed by integration. Intramolecular atomic distances and coupling constants were calculated by following guidelines in the MacroModel documentation.

One-Dimensional ^{1}H Spectrum. Parameters included the following: TD = 32K; AQ = 2.719; SI = 32K; SF = 500.13; O1 = 7421.68; SW = 6024.09; RG = 400.

Two-Dimensional XHCORR Spectrum. Parameters included the following: SI2 = 2048w; SI1 = 1024w; SW2 = 18518.519 Hz; SW1 = 1899.696 Hz; D1 = 1.2; S1 = 1H; P1 = 17.0; D0 = 0.0000030; P4 = 15.60; D3 = 0.0040; P3 = 7.80; D4 = 0.0012; S2 = 18H; RD = 0.0; PW = 0.0; DE = 10.00; NS = 80; DS = 2; P9 = 110.00; NE = 512; IN = 0.0001316. Two-dimensional Fourier transform and display parameters included WDW2 = G, WDW1 = G, LB2 = 2.0, GB1 = 0.0, and GB2 = 0.0.

Two-Dimensional DQFCOSYPH Spectra. Absorption mode spectra were collected in the TPPI mode. Parameters for the full sweep width spectrum (δ 7.7 → 0.7) included the following: O1 = 7524.635; O2 = 0.0; NS = 16; DS = 2; NE = 512; TD2 = 4K; TD1 = 512W; SI2 = 4K; SI1 = 1K; SF2 = 500.13; SF1 = 500.13; SW2 = 3521.127; SW1 = 1760.563. Two-dimensional Fourier transform and display parameters included the following: WDW2 = S; WDW1 = S; LB2 = 0.0; LB1 = 0.0; GB2 = 0.0; GB1 = 0.0.

Parameters for the δ 5.5 → 1.8 shift range were the same as above with the following adjustments: O1 = 7268.835, SW = 1858.736. Parameters for the δ 5.0 → 0.9 shift range were the same as above with the following adjustments: O1 = 6915.754, SW = 2049.180.

DISCO Additions. Projections of cross peaks from the limited sweep width DQFCOSYPH experiments were generated via the Bruker DISCO subroutine in the AP2D submode. The resultant 4K projections were inverse Fourier transformed, zero-filled to 16K, and then retransformed to projections with ca. 0.2 Hz digital resolution. Subsequent additions of the derived projections were performed in the Bruker dual display mode.

NOE Study.[20b] Parameters for the NOE study included the following: DP = 25L; TD = 16K; SI = 16K; SF = 500.13; SW = 6024.096; NS = 512; RD = 0.0; PW = 8.0; RG = 640.

Acknowledgment. We are pleased to acknowledge support of this investigation by the National Institutes of Health (National Cancer Institute) through Grant CA-19033. Dr. Christopher S. Shiner provided helpful suggestions and critical comments.

Registry No. 1, 77642-19-4.

Supplementary Material Available: Tables of X-ray data for hitachimycin, ^{1}H (500 MHz) and ^{13}C (125 MHz) NMR chemical shift assignments of hitachimycin, and the Monte Carlo command file and 500-MHz ^{1}H NMR PANIC simulation spectra of hitachimycin (11 pages). Ordering information is given on any current masthead page.